Mechanism of Alkyne Insertion into the Ru−C Bonds of Orthoruthenated Compounds Featuring Similarity of the Ru(II) and Pd(II) Reactions

Wolfgang Ferstl,[†,1] Inna K. Sakodinskaya,[‡] Nohma Beydoun-Sutter,[§] Guy Le Borgne,[∥] Michel Pfeffer,[§] and Alexander D. Ryabov*[,†,‡,2]

Division of Chemistry, G. V. Plekhanov Russian Economic Academy, Stremyanny per. 28, 113054 Moscow, Russia, Department of Chemistry, Moscow State University, 119899 Moscow, Russia, Université Louis Pasteur, Laboratoire de Synthèses Métallo-induites, URA 416 du CNRS, 4 rue Blaise Pascal, 67070 Strasbourg Cedex, France, and Laboratoire de Cristallochimie, Université de Rennes, URA 254 du CNRS, 35042 Rennes Cedex, France

Received August 8, 1996[⊗]

The pseudo-first-order rate constants k_{obs} for the reaction between the ring-substituted orthoruthenated *N*,*N*-dimethylbenzylamines [$Ru^{II}(\eta^6\text{-}C_6H_6)(o\text{-}C_6H_3RCH_2NMe_2)Cl$] (R = 4,5-$(MeO)_2$, 5-Me, H, 5-F), and alkynes R′C≡CR″ (R′/R″ = Ph/Ph, Ph/$C_6H_4CF_3$-3, Ph/$C_6H_4NO_2$-4, Et/Et, CO_2Me/CO_2Me) to afford the isoquinolinium cations coordinated to the [$Ru^0(\eta^6\text{-}C_6H_6)$] moiety are a linear function of [R′C≡CR″] in methanol at 20.0−40.0 °C in accord with the rate-determining insertion of alkyne into the Ru−C bond. The latter was confirmed by the observation that the electron-donating groups R at the dimethylbenzylamine ruthenocycle favor the insertion and the slope of the corresponding Hammett plot equals −1.6 against σ^+. The electron-poor alkynes react slower than the electron-rich ones. An X-ray structural investigation of the product of the $MeO_2CC{\equiv}CCO_2Me$ reaction with the related ruthenocycle [(3-MeC_5H_3N-2-C_6H_4)Ru(μ-I)$(CO)_2$]$_2$ demonstrates that the alkyne inserts into the Ru−C bond. Addition of LiCl retards the insertion markedly indicative of the importance of the ionization of the coordinated chloride. The major reaction pathway involves the solvento species [$Ru^{II}(\eta^6\text{-}C_6H_6)(o\text{-}C_6H_3RCH_2NMe_2)(MeOH)]^+$, the existence of which was confirmed by the spectrophotometric study of the starting compound in the presence of LiCl. All the observations reported show that the d^6 system under study is very mechanistically similar to the insertion of alkynes into the dinuclear d^8 Pd^{II} complexes [Pd($o\text{-}C_6H_3RCH_2\text{-}NMe_2$)($\mu$-Cl)]$_2$, the key difference being the ways of creation of a coordinative site readily accessible by alkyne. These are the ionization of the Ru−Cl bond and the cleavage of the [Pd(μ-Cl)$_2$Pd] bridge in the ruthenium and palladium cases, respectively.

Introduction

Insertion of alkynes into the transition metal−carbon bonds is nowadays a rapidly growing area of the transition metal chemistry[3] at the interface of organometallic chemistry, homogeneous catalysis, and fine organic synthesis. A great synthetic potential of orthopalladated compounds for the preparation of diverse heterocycles was demonstrated in the last decade.[4] Remarkably, orthometalated systems other than based on d^8 palladium(II) complexes have recently been also proposed, among which d^6 ruthenium(II) complexes **1** seem to be the most promising[5] as they also lead to the formation of heterocycles in the presence of alkynes. The mechanism that might take place involves either the insertion into the Ru−C bond or the nucleophilic addition of the amino group to the alkyne to afford intermediate **2** or **3**, respectively, followed by the reductive elimination step resulting in the formation of complexes **4** with the isoquinolinium cations η^4-coordinated to the [$Ru^0(\eta^6\text{-}C_6H_6)$] moiety, Scheme 1.

The process is worth detailed mechanistic study for these two reasons. First, there are no similar examples in the literature where the ready alkyne insertion is followed by the reductive elimination step to afford the heterocyclic product under extremely mild conditions. There is indeed a related alkyne insertion followed by the reductive elimination involving [bis(((dimethyl-

[†] G. V. Plekhanov Russian Economic Academy.
[‡] Moscow State University.
[§] Université Louis Pasteur.
[∥] Université de Rennes.
[⊗] Abstract published in *Advance ACS Abstracts,* January 1, 1997.

(1) IAESTE exchange student; on leave from the University of Regensburg, Regensburg, FRG.

(2) E-mail: ryabov@enzyme.chem.msu.su.

(3) See, for example: Ricci, J. S.; Ibers, J. A. *J. Organomet. Chem.* **1971**, *27*, 261. Bruce, M. I.; Gardner, R. C. F.; Stone, F. G. A. *J. Chem. Soc., Dalton Trans.* **1976**, 81. Wu, G.; Rheingold, A. L.; Heck, R. F. *Organometallics* **1987**, *6*, 2386. Wu, G.; Geib, S. J.; Rheingold, A. L.; Heck, R. F. *J. Org. Chem.* **1988**, *53*, 3238. Dupont, J.; Pfeffer, M.; Daran, J. C.; Gonteron, J. *J. Chem. Soc., Dalton Trans.* **1988**, 2421. Tao, W.; Silverberg, L. J.; Heck, R. F. *Organometallics* **1989**, *8*, 2550. Liebeskind, L. S.; Gasdaska, J. R.; McCallum, J. S. *J. Org. Chem.* **1989**, *54*, 669. Albert, J.; Granell, J.; Sales J. *J. Organomet. Chem.* **1989**, *379*, 177. Pfeffer, M.; Rotteveel, M. A.; Sutter, J. P.; De Cian, A.; Fischer, J. *J. Organomet. Chem.* **1989**, *371*, C21. Sutter, J. P.; Pfeffer, M.; De Cian, A.; Fischer, J. *Organometallics* **1992**, *11*, 386.

(4) For a review, see: (a) Pfeffer, M. *Rec. Trav. Chim. Pays-Bas* **1990**, *109*, 567. For more recent leading references, see: (b) Spencer, J.; Pfeffer, M.; Kyritsakas, N.; Fischer, J. *Organometallics* **1995**, *14*, 2214. Spencer, J.; Pfeffer, M.; Kyritsakas, N.; Fischer, J. *J. Org. Chem.* **1995**, *60*, 1005. Maassarani, F.; Pfeffer, M.; Spencer, J.; Wehman, E. *J. Organomet. Chem.* **1994**, *466*, 265. Vicente, J.; Abad, J.-A.; Gil-Rubio, J.; Jones, P. G. *Organometallics* **1995**, *14*, 2677. Vicente, J.; Abad, J.-A.; Bergs, R.; Jones, P. G.; de Arrelano, M. C. R. *Organometallics*, **1996**, *15*, 24. Vicente, J.; Abad, J.-A.; Fernande-de-Bobadilla, R.; Jones, P. G.; de Arrelano, M. C. R. *Organometallics* **1996**, *15*, 1422.

(5) Abbenhuis, H. C. L.; Pfeffer, M.; Sutter, J.-P.; de Cian, A.; Fischer, J.; Ji, H. L.; Nelson, J. H. *Organometallics* **1993**, *12*, 4464.

S0276-7333(96)00674-7 CCC: $14.00

Scheme 1

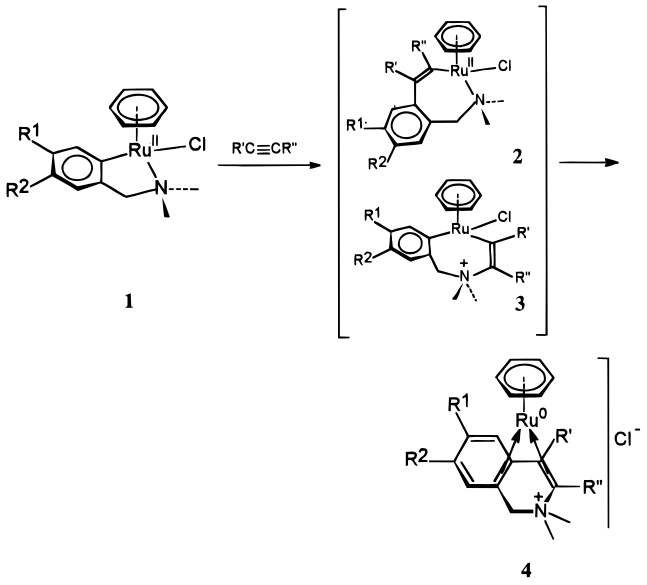

R^1/R^2 = H/H (a), MeO/MeO (b), Me/H (c), F/H (d)

R'/R" = Ph/Ph, Ph/$C_6H_4CF_3$-3, Ph/$C_6H_4NO_2$-4, Et/Et, CO_2Me/CO_2Me

Scheme 2

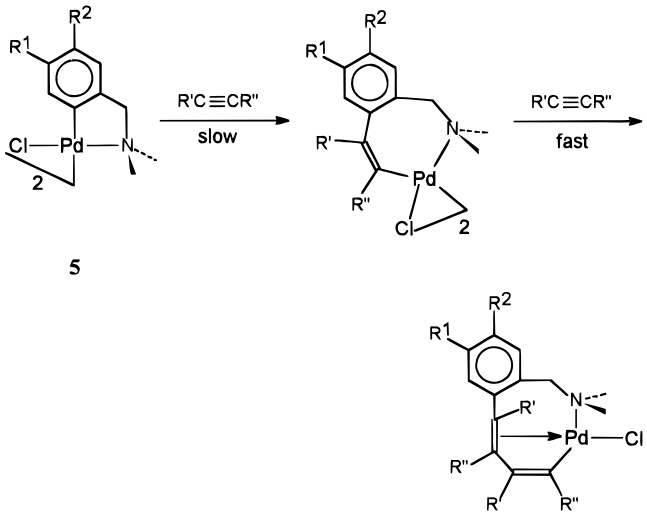

amino)methyl)naphthalenato-*C,N*)palladium(II)][6] which, however, occurs at refluxing chlorobenzene and thus is less suitable for a mechanistic study. Second, we have recently studied the mechanism of alkyne insertion into the Pd−C bonds of similarly substituted *N,N*-dimethylbenzylamine complexes **5**, Scheme 2,[7] and it is interesting to compare the major mechanistic features of the alkyne insertion reactions involving the d^6 Ru^{II} and d^8 Pd^{II} complexes. Therefore, in this paper we report the results of detailed kinetic study of the insertion of alkynes into the Ru−C bonds of ring-substituted *N,N*-dimethylbenzylamine complexes **1**. Since the kinetics are silent in terms of choosing between the intermediates **2** and **3**, an X-ray structural study of **7** has been invoked to prove that the Ru−C bond is the main gate in the coordination sphere of Ru^{II}. The data obtained are compared with the corresponding kinetic data on reactions of the palladacycles **5** and nickelacycles [Ni(*o*-$C_6H_4CH_2PPh_2$)(μ-Cl)]$_2$[8] primarily with alkynes, although the relevant kinetic information on reactions of the palladium complexes with alkenes[9] has also been invoked.

(6) Beydoun, N.; Pfeffer, M. *Synthesis* **1990**, 729.

(7) Ryabov, A. D.; van Eldik, R.; Le Borgne, G.; Pfeffer, M. *Organometallics* **1993**, *12*, 1386.

(8) Martinez, M.; Muller, G.; Panyella, D.; Rocamora, M.; Solans, X.; Font-Bardía, M. *Organometallics* **1995**, *14*, 5552.

(9) (a) Ryabov, A. D.; Sakodinskaya, I. K.; Yatsimirsky, A. K. *J. Chem. Soc., Perkin Trans. 2* **1983**, 1511. (b) *J. Organomet. Chem.* **1991**, *406*, 309.

(10) Pfeffer, M.; Sutter, J. P.; Urriolabeitia, E. *Inorg. Chim. Acta* **1996**, *249*, 63.

Experimental Section

Reagents. Diphenylethyne and hex-3-yne were obtained from Aldrich. Phenyl(4-nitrophenyl)ethyne and phenyl(3-(trifluoromethyl)phenyl)ethyne were synthesized as described previously.[6] Dimethyl acetylenedicarboxylate (DMAD) was an Aldrich preparation. ((Dimethylamino)methyl)benzene and 1-(dimethylamino)methyl-3,4-dimethoxybenzene were purchased from Aldrich. The corresponding 4-methyl and 4-fluorine derivatives obtained as described elsewhere.[10] Ruthenium complexes **1** were prepared as described previously.[5] Methanol (Chimed) used as solvent was refluxed over CaH_2 for 2 h and then distilled. Lithium chloride (Reakhim) was dried at 120 °C overnight before use.

Synthesis of [(3-MeC_5H_3N-2-C_6H_4)Ru(μ-Cl)$(CO)_2$]$_2$ (6a). $RuCl_3 \cdot 3H_2O$ (4 g, 15.3 mmol) was dissolved in 2-methoxyethanol (100 mL). Carbon monoxide was bubbled in the dark through a blue solution at reflux for 8 h leading to a yellow solution. An excess of 2-phenyl-3-methylpyridine (8 g, 45 mmol) was then added at room temperature, and after the solution was stirred at reflux for 1.5 h, **6a** was obtained as a pale yellow precipitate. It was filtered out and washed with diethyl ether and *n*-pentane (yield 4.41 g, 80%). Anal. Calcd (found) for $C_{14}H_{10}ClNO_2Ru$ (M_r 360.76): C, 46.61 (47.21); H, 2.79 (2.86); N, 3.88 (3.83).

Synthesis of [(3-MeC_5H_3N-2-C_6H_4)Ru(μ-I)$(CO)_2$]$_2$ (6b). Compound **6a** (1.04 g, 1.44 mmol) in acetone was treated under reflux in the presence of ca. 5-fold excess of NaI for 5 h leading to a deep yellow solution. After removal of acetone *in vacuo*, **6b** was extracted in CH_2Cl_2 and precipitated with *n*-hexane as a yellow powder (1.195 g, 92%). Anal. Calcd (found) for $C_{14}H_{10}INO_2Ru$ (M_r 452.22): C, 37.18 (37.76); H, 2.23 (2.13); N, 3.09 (2.95).

Synthesis of [(3-MeC_5H_3N-2-C_6H_4($MeO_2CC{=}CCO_2Me$))-RuI$(CO)_2$(4-MePy)] (7). To a solution of **6b** (0.452 g, 0.39 mmol) in chlorobenzene (30 mL) was added DMAD (0.284 g, 2 mmol). The green solution was slowly heated to 80 °C under continuous stirring until it turned dark yellow. After removal of the solvent *in vacuo*, the residue was redissolved in the minimum amount of CH_2Cl_2, and *n*-hexane was added to the filtrate affording a yellow powder which was washed with *n*-hexane and dried *in vacuo* (0.487 g, 90%). 4-Methylpyridine was added to a solution of the latter in CH_2Cl_2 leading to a pale yellow solution. Slow diffusion of *n*-hexane into this solution at −20 °C afforded yellow crystals of **7** after 12 h. Anal. Calcd (found) for $C_{26}H_{23}IN_2O_6Ru$ (M_r 687.96): C, 45.43 (44.90); H, 3.38 (3.39); N, 4.07 (4.02). ^{1}H NMR ($CDCl_3$, δ): 8.54 (d, 1 H arom, $^3J_{HH}$ 6.0), 7.75 (d, 1 H arom, $^3J_{HH}$ 7.5), 7.49−7.00 (m, 9 H arom), 6.61 (d, 1 H arom, $^3J_{HH}$ 7.7), 3.79 and 3.69 (2s, 6 H, $2OCH_3$), 2.40 and 2.21 (2s, 6 H, $2CH_3$). ^{13}C NMR ($CDCl_3$, δ): 155.6, 153.4, 140.9, 131.7, 130.9, 129.4, 127.7, 125.1, 122.7 (aromatic C−H), 52.0 and 50.9 (OCH_3), 21.4 and 21.2 (CH_3). IR (KBr, cm^{-1}): ν(C≡O) 2046, 1985; ν(C═O) 1706.

Kinetic and Other Measurements. The reactions at 20−40 °C were studied spectrophotometrically on a Shimadzu UV-160A instrument equipped with a temperature-controlled (±0.1 °C) cell compartment providing six independent measurements. Reaction kinetics was studied at 450 nm in the case of **1a**,**c** and at 440 nm in the case of **1b**,**d**. These wavelengths were chosen to achieve the highest spectral changes. The

Table 1. Summary of Crystal Data and Intensity Collection of 7

chemical formula	$C_{26}H_{23}IN_2O_6Ru$
cryst syst	monoclinic
space group	$P2_1/n$
a, Å	9.591(2)
b, Å	14.261(9)
c, Å	19.626(3)
β, deg	100.94
V, Å^3	2635.6
M_r, g/mol	687.46
Z	4
cryst dimens, mm	0.39 × 0.36 × 0.32
λ(Mo Kα), Å	0.710 73
μ, cm^{-1}	17.8
F(000)	1352
scan range, deg	1.00 + 0.35 tan θ
θ limits, deg	1−25
no. of reflcns, total	5139
no. of reflcns, used	3900 ($I > 3\sigma(I)$)
R factor, %	0.031
R_w factor, %	0.046
std error in an observn of unit weight, e	1.57

pseudo-first-order conditions were ensured by using a large excess (at least 10-fold) of alkyne compared to **1**. The reactions were started by adding the required amount of the stock solution of alkyne in MeOH into a 1 cm quartz cuvette equipped with a Teflon stopper containing complex **1** dissolved in MeOH. The commonly used concentration of compounds **1** was 0.037 × 10^{-2} M. Concentrations of alkynes were varied in the range (0.42−3.8) × 10^{-2} M. The k_{obs} values were evaluated by fitting the kinetic traces to the equation $A(t) = A_\infty + (A_0 - A_\infty)\{\exp(-k_{obs}t)\}$, where A_0 and A_∞ are the initial and final absorbances, respectively. By the example of complex **1a** it was verified that k_{obs} are nearly independent on [**1**] in the range (3.7−14.0) × 10^{-4} M. A stock solution of phenyl(4-nitrophenyl)ethyne was prepared in chloroform and then added to the solution of **1a** in MeOH. The total amount of $CHCl_3$ in the system was 9% (v/v). The rate constants shown throughout the paper are the mean values of at least three measurements. The curve fit and all other calculations were performed using a Sigma Plot 1.0 package.

Crystal Structure Determination of 7. Intensities were measured on an Enraf-Nonius CAD-4 diffractometer. The crystal parameters and a summary data collection and structure refinement are given in Table 1. No intensity decay was observed during the data collection period. Corrections for the Lorentz and polarization effect were applied but not for absorption owing to the low value of the linear absorption coefficient.

All the calculations were performed on a microVax 3100 computer using the Molen program.[11] The atomic positions of the independent non-hydrogen atoms were found with the program MUTAN and the subsequent Fourier difference synthesis. Refinement of coordinates and thermal parameters, first isotropic and then anisotropic, of the 36 independent atoms led to the final R values reported in Table 1.

Results

General Observations, Rate Law, and Substituent Effects. The reaction between complexes **1** and diphenylethyne occurs readily in MeOH as solvent, and this medium has been chosen for kinetic spectrophotometric measurements. The spectral changes that follow the conversion of **1** into **4** in an excess of [PhC≡CPh] are presented in Figure 1a,b by the example of complex **1a** both in the absence and in the presence of LiCl, respectively. Under such conditions, even at lower relative concentrations of diphenylethyne, the reaction is complete in a matter of ca. 30 min at [LiCl] = 0 according to the ^{1}H NMR data, the yield of **4** exceeding 90%. This makes the system very convenient for systematic kinetic study by following a decrease in absorbance at ca. 450 nm.

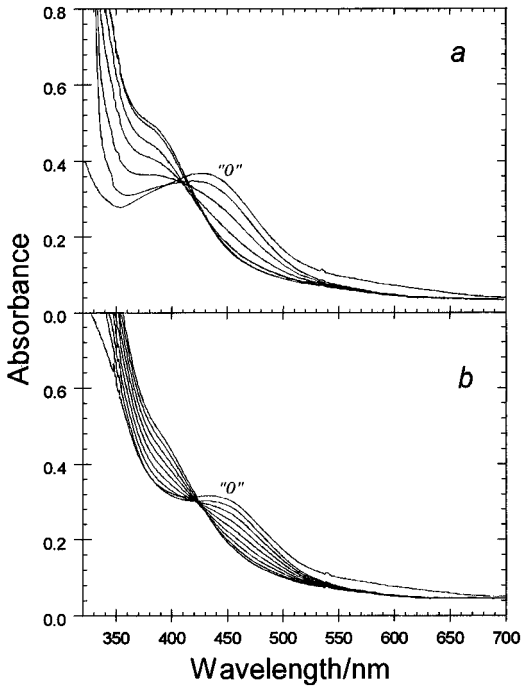

Figure 1. Spectral changes during the reaction between **1a** (3.7 × 10^{-4} M) and diphenylethyne (85 × 10^{-4} M) in MeOH at 25 °C. (a) In the absence of LiCl. Spectrum "*0*" is without diphenylethyne; other spectra were run after 0.33, 2, 5, 10, 20, and 40 min of addition of diphenylethyne. (b) In the presence of 0.01 M LiCl. Spectrum "*0*" was recorded without diphenylethyne; other spectra were run after 0.42, 5, 11, 19, 29, 42, 62, and 92 min.

The spectral patterns that accompany the reaction progress show a diversity, if the process is run in the absence and in the presence of LiCl. As can be seen by comparing Figure 1a,b, the reaction is faster in the absence of chloride, and no isosbestic point is observed on the rearrangement of **1** into **4**. Lithium chloride seems to improve the spectral pattern by visualizing the isosbestic point. These qualitative observations suggest that more than two species are present in solution.

Good pseudo-first-order behavior was observed for reactions of all complexes **1** with diphenylethyne. The values of k_{obs} showed no variation for at least 4−5 half-lives and were essentially independent of the initial concentration of complexes **1**. The values of k_{obs} determined at different concentrations of diphenylethyne in the temperature range 20−40 °C are summarized in Table 2, while the corresponding enthalpy and entropy of activation can be found in Table 3. The dependence of k_{obs} for **1a**−**d** on concentration of diphenylethyne showing the first-order dependence in the incoming alkyne is demonstrated in Figure 2. The corresponding rate low is given in (1). The strict first order in

$$k_{obs} = k_2[RC{\equiv}CR] \qquad (1)$$

diphenylethyne is a strong support for the rate-determining insertion of alkyne into the Ru−C or Ru−N bond of **1** to afford intermediate **2** or **3**, respectively,

(11) Fair, C. K. Molen. An Intercative Intelligent System for Crystal Structure Analysis. Enraf-Nonius, Delft, The Netherlands, 1990.

Table 2. Complete k_{obs} Values for Reactions of Complexes 1 with PhC≡CPh in MeOH

run	complex (R^1/R^2)	10^2[PhC≡CPh]/M	T/°C	$10^2 k_{obs}/s^{-1}$	$k_2/M^{-1}\ s^{-1}$
1	**1a** (H/H)	0.85	20	0.20 ± 0.01	0.21 ± 0.04
2		1.7		0.38 ± 0.03	
3		2.98		0.54 ± 0.02	
4		3.8		0.88 ± 0.03	
5		0.42	25	0.20 ± 0.05	0.35 ± 0.01
6		0.85		0.42 ± 0.01	
7		1.2		0.51 ± 0.05	
8		1.7		0.69 ± 0.06	
9		2.1		0.84 ± 0.04	
10		2.98		1.10 ± 0.03	
11		3.8		1.36 ± 0.04	
12		0.45	30	0.30 ± 0.10	0.63 ± 0.07
13		0.85		0.57 ± 0.02	
14		1.2		0.87 ± 0.02	
15		1.7		1.07 ± 0.17	
16		0.42	35	0.50 ± 0.03	0.92 ± 0.05
17		0.85		1.01 ± 0.04	
18		1.2		1.41 ± 0.05	
19		1.7		1.64 ± 0.09	
20		2.98		2.82 ± 0.04	
21		0.42	40	0.68 ± 0.04	1.56 ± 0.16
22		0.85		1.23 ± 0.14	
23		1.2		2.21 ± 0.30	
24		1.7		2.51 ± 0.23	
25	**1d** (F/H)	1.7	20	0.20 ± 0.01	0.10 ± 0.01
26		2.1		0.25 ± 0.01	
27		2.98		0.30 ± 0.01	
28		3.8		0.38 ± 0.01	
29		0.42	25	0.09 ± 0.02	0.16 ± 0.02
30		1.2		0.22 ± 0.02	
31		2.1		0.45 ± 0.09	
32		3.8		0.61 ± 0.05	
33		1.7	30	0.54 ± 0.04	0.27 ± 0.02
34		2.1		0.58 ± 0.04	
35		2.98		0.77 ± 0.05	
36		3.8		1.08 ± 0.01	
37	**1c** (Me/H)	0.85	20	0.38 ± 0.02	0.47 ± 0.02
38		1.2		0.54 ± 0.01	
39		1.7		0.76 ± 0.05	
40		2.1		1.01 ± 0.03	
41		0.42	25	0.31 ± 0.02	0.73 ± 0.03
42		0.85		0.60 ± 0.03	
43		1.2		0.89 ± 0.07	
44		1.7		1.06 ± 0.12	
45		2.1		1.5 ± 0.2	
46		2.98		2.25 ± 0.52	
47		0.42	30	0.52 ± 0.02	1.15 ± 0.04
48		0.85		1.07 ± 0.07	
49		1.2		1.36 ± 0.19	
50		1.7		1.97 ± 0.04	
51	**1b** (MeO/MeO)	0.34	25	1.43 ± 0.09	4.91 ± 0.02
52		0.42		1.75 ± 0.06	
53		0.51		2.28 ± 0.37	
54		0.68		3.42 ± 0.16	

Table 3. Enthalpies and Entropies of Activation, $\Delta H^{\ddagger}$ and $\Delta S^{\ddagger}$, for Reactions of Diphenylethyne with Ru^{II} Complexes 1 and Pd^{II} Complexes 5[7] Having Different Substituents in the *N*,*N*-Dimethylbenzylamine Ring in MeOH and $CHCl_3$ Solvents, Respectively

	Ru complexes **1**		Pd complexes **5**	
R^1/R^2	$\Delta H^{\ddagger}$/kJ mol^{-1}	$\Delta S^{\ddagger}$/J mol^{-1} K^{-1}	$\Delta H^{\ddagger}$/kJ mol^{-1}	$\Delta S^{\ddagger}$/J mol^{-1} K^{-1}
F/H	71 ± 3	−22 ± 10	71 ± 1	−47 ± 5
H/H	73 ± 3	−7 ± 10	50 ± 2	−99 ± 6
Me/H	63 ± 1	−34 ± 2	50 ± 4	−97 ± 12

which transforms then rapidly into the final product **4**. The pronounced substituent effect brought about by R^1 and R^2 in the *N*,*N*-dimethylbenzylamine fragment of **1**, which results in an increase in k_{obs} for the electron-rich species, rules out alkyne π-complex formation with d^6 ruthenium(II) complexes as a rate-limiting step, since the opposite reactivity trend should be expected in the latter case. The k_2 values follow the Hammett equation, the analytical form of which is $\log k_2 = (-1.24 \pm 0.05) + (-1.6 \pm 0.2)\sigma^+$. The slope of the plot of −1.6 should be compared with that of −2.2 observed previously for the insertion of diphenylethyne into the Pd−C bond of similarly substituted orthopalladated *N*,*N*-dimethylbenzylamine complexes **5**, which follow absolutely identical rate law (1). In contrast to the substituent effect in **1**, that in alkynes is less pronounced (Table 4), but it indicates that the electron-withdrawing groups slow down the insertion marginally.

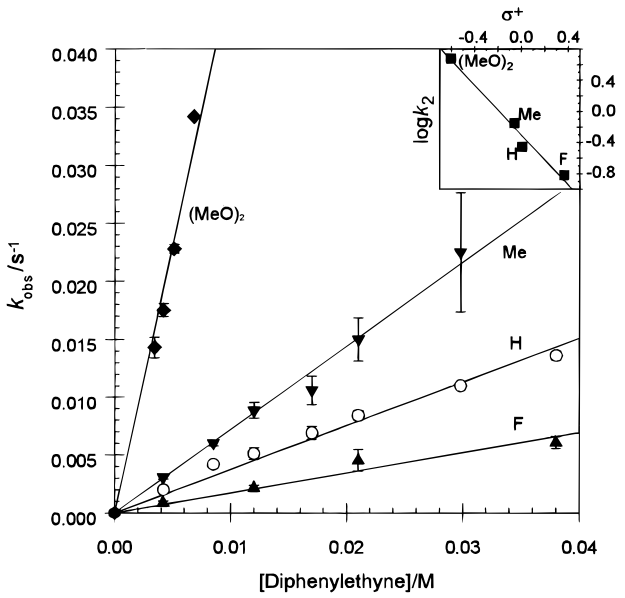

Figure 2. Pseudo-first-order rate constants k_{obs} for reactions of the ring-substituted complexes **1a**−**d** as a function of [PhC≡CPh] in MeOH at 25 °C. Inset: Hammett plot for the second-order rate constants k_2.

Table 4. Values of k_{obs} for Reactions of Different Alkynes with 1a at 25 °C, with [1a] = 3.7×10^{-4} M and [Alkyne] = 0.017 M

run	alkyne	$10^2 k_{obs}/s^{-1}$
1	diphenylethyne	0.69 ± 0.05
2	hex-3-yne	0.76 ± 0.10
3	phenyl(3-trifluorophenyl)ethyne	0.20 ± 0.01
4	phenyl(4-nitrophenyl)ethyne	0.30 ± 0.01
5	DMAD	0.37 ± 0.02

X-ray Structural Evidence for Intermediate 2. There are not many examples of insertion of alkynes into Ru−C bonds available in the literature.[12] Nevertheless, we have a further evidence for the alkyne insertion into the Ru−C bond of ruthenocycles as we could isolate such a compound using however another Ru complex **6b** (see Scheme 3). The synthesis of a compound closely related to **6a** with cycloruthenated 2-phenylpyridine was described a long time ago,[13] but

(12) Lutsenko, Z. L.; Aleksandrov, G. G.; Petrovskii, P. V.; Shubina, E. S.; Andrianov, V. G.; Struchkov, Yu. T.; Rubezhov, A. Z. *J. Organomet. Chem.* **1985**, *281*, 349. Crook, J. R.; Chamberlain, B.; Hawby, R. J. *J. Chem. Soc., Dalton Trans.* **1989**, 465. Bruce, M. I.; Catlow, A.; Cifuentes, M. P.; Snow, M. R.; Tiekink, E. T. R. *J. Organomet. Chem.* **1990**, *397*, 187. Echavarren, A. M.; Lopez, J.; Santos, A.; Montoya, J. *J. Organomet. Chem.* **1991**, *414*, 393. Castano, A. M.; Echavarren, A. M.; Lopez, J.; Santos, A. *J. Organomet. Chem.* **1986**, *379*, 171.

(13) Hiraki, K.; Obayashi, Y.; Oki, Y. *Bull. Chem. Soc. Jpn.* **1979**, *52*, 1372.

Scheme 3

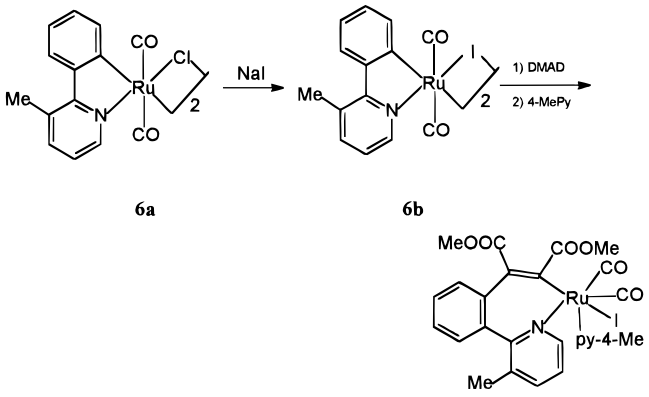

Table 5. Selected Bond Distances (Å) and Angles (deg) for Complex 7

Bond Distances			
Ru−N1	2.175 (3)	C12−C13	1.342 (4)
Ru−N2	2.193 (3)	C11−C12	1.486(4)
Ru−C13	2.074 (3)	C5−C6	1.500 (4)
Ru−C25	1.883 (4)	C13−C16	1.489 (4)
Ru−C26	1.854 (4)	C12−C14	1.497 (4)
Ru−I	2.7968 (3)		

Bond Angles			
N1−Ru−N2	87.5 (1)	N1−Ru−C13	88.7 (1)
N1−Ru−I	90.88 (7)	N2−Ru−I	89.99(7)
C25−Ru−C26	87.0(2)	C13−Ru−N1	88.7(1)
Ru−N1−C5	124.4(2)	N1−C5−C6	120.1(3)
C5−C6−C11	126.5(3)	C6−C11−C12	123.6(3)
C11−C12−C13	124.1(3)	C12−C13−Ru	128.2(2)

to our knowledge, no reactivity studies have ever been performed with it. We found that the chloride derivative **6a** was unreactive with internal alkynes whereas the corresponding iodo-bridged dimer **6b** reacted with DMAD readily. This reaction afforded an iodo-bridged dimer the ^{1}H NMR spectrum of which was very complex. However, the monomeric compound **7** was readily formed in the presence of 4-methylpyridine, its ^{1}H NMR spectrum was more easy to interpret, and, in addition, crystals of **7** suitable for an X-ray diffraction study could be obtained.

The crystal structure of **7** has thus been determined, and a view of the molecule is shown in Figure 3. As seen, the reaction ends up with the alkyne insertion into the *Ru−C* bond. Selected bond distances and bond angles are shown in Table 5. The geometry around the Ru atom is that of a slightly distorted octahedron whereas the seven-membered organometallic ring has features (bond distances and angles) very similar to those of related palladium derivatives.[14]

Effect of Lithium Chloride on k_2. As mentioned above, LiCl affects the course of alkyne insertion and, therefore, the k_2 for the interaction of **1a** and diphenylethyne were obtained at different [LiCl]. The data shown in Figure 4, where k_2 are plotted against the total concentration of LiCl, clearly indicate that the rate is strongly retarded in the presence of the salt. The strong rate inhibition by chloride was also observed in the palladium(II) case shown in Scheme 2 and ascribed to the formation of the unreactive monomeric cis-di-

(14) See, for example: Arlen, C.; Pfeffer, M.; Bars, O.; Grandjean, D. *J. Chem. Soc., Dalton Trans.* **1983**, 1535.

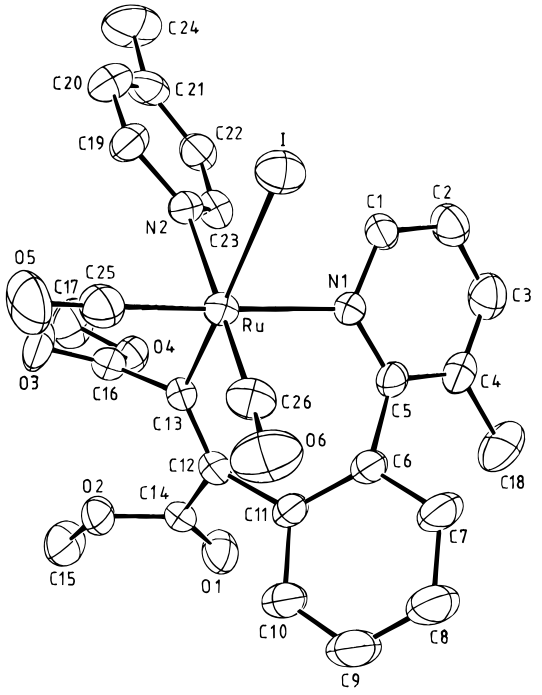

Figure 3. Crystal structure of complex **7**.

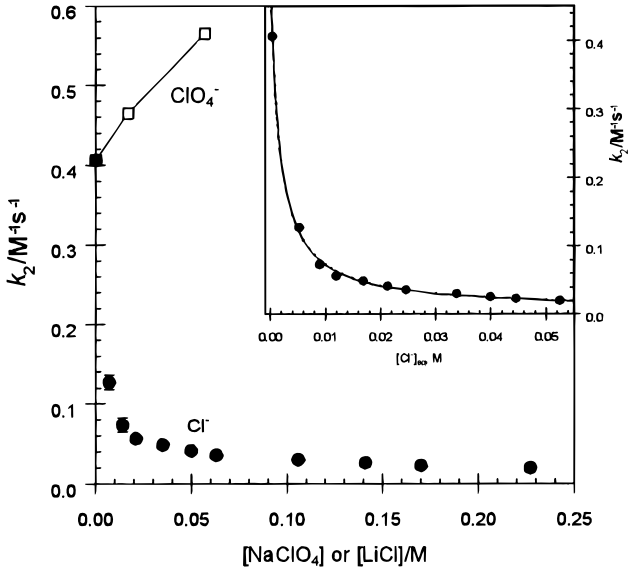

Figure 4. Effect of LiCl and $NaClO_4$ on the rate constants k_2 for insertion of PhC≡CPh into Ru−C bond of **1a** in MeOH at 25 °C. [**1a**] = 3.7×10^{-4} M, and [PhC≡CPh] = 1.7×10^{-2} M. Inset: Rate constants plotted against calculated concentration of Cl^-. The solid line is the calculated dependence using the best fit values of k_s, k_{Cl}, and K_{Cl}.

chloropalladium(II) species $[(C^{\frown}N)PdCl_2]^-$ in $CHCl_3$ solvent[7] where $(C^{\frown}N)^-$ stands for an orthopalladated ligand.

Naturally, similar monomerization cannot be invoked in the present ruthenium case, since the starting complexes **1** are the coordinatively saturated monomeric species. It is thus more probable to assume that the reactive solvento species are produced via the ionization of the Ru−Cl bond in complexes **1**. As a result, the incorporation of alkyne into the coordinative sphere of Ru(II) by substituting a methanol molecule rather than chloride becomes much easier. The ionization affording the cationic ruthenium(II) species does not seem un-

Scheme 4

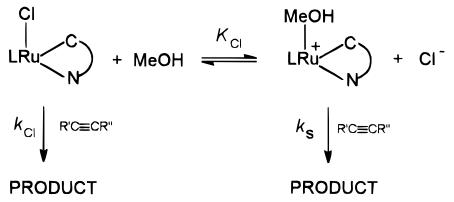

likely, since the reactions are run in polar methanol solvent in which the ionization of various electrolytes is a matter of common knowledge.[15] Therefore, a plausible stoichiometric mechanism corresponding to the data shown in Figure 4 could be as in Scheme 4, where L stands for η^6-C_6H_6. The corresponding expression for k_2 is given by eq 2, where [Cl^-] is the equilibrium concentration of chloride in MeOH solution. It is important to note that the data shown in Figure 4 should be analyzed taking into account the known value for the dissociation constant of LiCl (K_{LiCl}) in MeOH of 1.58×10^{-2} M,[15] since the kinetic data were evaluated in the 0.007−0.14 M range of [LiCl]. Therefore, the equilibrium concentrations of Cl^- were calculated using the K_{LiCl} value which were then used in the fitting of the experimental data to eq 2. The contribution of Cl^- from dissociated complex **1**, which was neglected in calculation of the equilibrium [Cl^-] since its concentration was as low as 3.7×10^{-4} M, was used only once, when no external LiCl was added. It was learned from the fit that the contribution of the "chloride" pathway k_{Cl} into the overall reaction rate is insignificant but does improve the fit which is shown as inset in Figure 4. The resulting best fit value for the dissociation constant K_{Cl} equals $(1.6 \pm 0.1) \times 10^{-3}$ M, and those for the rate constants k_s and k_{Cl} equal 0.500 ± 0.009 and $(5.7 \pm 2.7) \times 10^{-3}$ M^{-1} s^{-1}, respectively. The numerical values of the rate constants indicate that only the "solvolytic" pathway governed by k_s plays a role in the reaction in Scheme 1, and the corresponding rate constant is close to the value for the experimentally measured rate constant k_2 shown in Table 2.

$$k_2 = \frac{k_s K_{Cl} + k_{Cl}[Cl^-]}{K_{Cl} + [Cl^-]} \qquad (2)$$

The known fact that the formation of **4** from **1** is also accessible in aprotic solvents in the presence of KPF_6 suggested the catalysis by an electrolyte. This was confirmed by speeding the reaction up by sodium perchlorate as shown in Figure 4.

Spectrophotometric Evidence for Chloride Dissociation. Figure 5 shows that the spectra of **1a** in MeOH are dependent on LiCl concentration as could be expected on the basis of the reaction mechanism in Scheme 4. It should be pointed out that the spectral changes are small and observed at total concentrations of LiCl comparable to that of **1a**. Therefore, extraction of K_{Cl} from the equilibrium data for the sake of its comparison with the value evaluated in the kinetic experiment becomes complicated. The spectral data were analyzed using the routine shortly described below. The absorbance in the range 400−450 nm is always

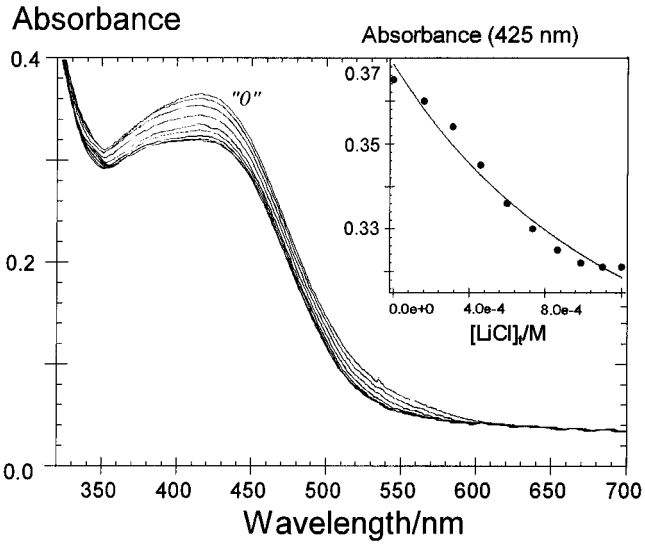

Figure 5. Spectral changes observed on addition of LiCl to the solution of **1a** in MeOH at 25 °C. The spectrum "*0*" is without LiCl; the next spectra were run in the presence of 1.6×10^{-4}, 3.1×10^{-4}, 4.6×10^{-4}, 6.0×10^{-4}, 7.4×10^{-4}, 8.6×10^{-4}, 9.9×10^{-4}, and 1.1×10^{-3} M LiCl. [**1a**] = 3.7×10^{-4} M. Inset: Absorbance change at 425 nm. The solid line represents the results of the data fitting using eqs 4 and 5.

given by eq 3, where ϵ are the exctinction coefficients

$$A = \epsilon_{Cl}[Ru_{Cl}] + \epsilon_s[Ru_s] \qquad (3)$$

with the subscripts indicating the corresponding participants in Scheme 4. Equation 3 may be rewritten as eq 4 taking into account both the mass balance equation

$$A = \epsilon_{Cl}[\mathbf{1}]_t - (\epsilon_{Cl} - \epsilon_s)[Ru_s] = \epsilon_{Cl}[\mathbf{1}]_t - (\epsilon_{Cl} - \epsilon_s)[\mathbf{1}]_t\left(\frac{K_{Cl}}{K_{Cl} + [Cl^-]}\right) \qquad (4)$$

with respect to the ruthenium species and the equilibrium in Scheme 4. The equilibrium chloride concentration [Cl^-] in eq 4 should be derived from the cubic eq 5 (see Appendix), since there is no excess of LiCl with respect to **1** in the spectrophotometric experiment and the concentrations of both are in fact comparable.

$$[Cl^-]^3 + (K_{Cl} + K_{LiCl})[Cl^-]^2 + (K_{Cl}K_{LiCl} - [\mathbf{1}]_t K_{Cl} - [LiCl]_t K_{LiCl})[Cl^-] - ([\mathbf{1}]_t + [LiCl]_t)K_{LiCl}K_{Cl} = 0 \qquad (5)$$

Analytical solution of eq 5 appeared to be rather ugly, and therefore, the experimental data were analyzed using a computer program adopted to this particular case.[16] The concentrations of [Cl^-] were computed at different K_{Cl} in the range $(1-4) \times 10^{-3}$ M. The resulting values of [Cl^-] and the corresponding K_{Cl} value were used in the fit of the absorbance vs [Cl^-] concentration according to eq 4 by varying ϵ_{Cl} and $(\epsilon_{Cl} - \epsilon_s)$ as fitting parameters. The minimum of the deviation functional[17] corresponded to the value of $K_{Cl} = (1.8 \pm 0.2) \times 10^{-3}$ M providing ϵ_{Cl} and ϵ_s equal 1050 and 660 M^{-1} cm^{-1}, respectively. The absorbance as a function of $[LiCl]_t$ calculated using the computed values is shown as inset

(15) Janz, C. J.; Tomkins, R. P. T. *Nonaqueous Electrolytes Handbook* Academic Press: New York, 1972.

(16) The computer program was made by Dr. A. V. Larin; it is available from the authors by request.

(17) Press, W. H.; Jeukosky, S. A.; Flannerry, B. P. *Numerical Recipes* Cambridge Press: Cambridge, U.K., 1992.

in Figure 5. The coincidence between the observed and calculated spectral data, as well as the correspondence between the values of K_{Cl} evaluated from the kinetic (1.6×10^{-3} M) and equilibrium experiments could be considered as acceptable taking into account the small spectral changes and different LiCl concentration ranges used in the two sets of experiments.

Discussion

The similarity between the kinetic features of the two alkyne insertion reactions shown in Schemes 1 and 2 is striking. The reactivity of the d^6 Ru^{II} complexes **1** and the d^8 Pd^{II} complexes **5**[7] is very close in terms of (i) the rate law (1) featuring the first-order kinetics in complex and alkyne, (ii) the substituent effect of groups R^1 and R^2 attached to the dimethylbenzylamine ring which results in the negative Hammett parameter ρ of ca. −2, (iii) close values of the enthalpy of activation (Table 3), and (iv) the pronounced retardation effect by added chloride. Observations i−iv clearly indicate similar mechanisms. However, it should be taken into account that the Ru and Pd insertions involve the monomeric and dimeric species and are run in polar methanol and aprotic chloroform solvents, respectively. The inhibition by chloride is strong evidence for the necessity of an accessible coordinative site for alkyne precoordination to the metal, but the two complexes realize different ways to achieve it in accordance with their chemical composition. It has been argued[7,18] that the labile bridge [Pd(μ-Cl)$_2$Pd] in complexes of type **5** represents an attractive entrance for ligands including alkynes into the coordinative sphere of Pd^{II}. Retardation by chloride in this case is due to the bridge cleavage to afford the coordinatively saturated anionic species $[(C\frown N)PdCl_2]^-$. Naturally, the "bridging" entrance cannot be realized in the case of monomeric complexes **1** in MeOH solvent. Hence, the major mechanistic difference between the Ru^{II} and Pd^{II} species concerns the alkyne access to the metal coordinative sphere which in the case of **1** is produced via the solvolysis of the chloro ligand as shown in Scheme 4. Alkynes, the affinity of which to organometallic Ru^{II} species is well documented,[19] are readily coordinated by the solvento species as shown in Scheme 5.

There are two pathways in Scheme 5, viz. the dominant "S-pathway" and much less important "Cl-pathway", which are driven by the experimentally evaluated rate constants k_s and k_{Cl}, respectively. In terms of the mechanism proposed, $k_s = K^s_{alkyne}k^s_{ins}$ and $k_{Cl} = K^{Cl}_{alkyne}k^{Cl}_{ins}$.

"S-Pathway". As it was already mentioned, the rate constants and activation parameters in Tables 2 and 3 correspond basically to the this solvolytic pathway. The fast reversible coordination of alkyne is the reaction that follows the solvolysis. The next step is the rate-limiting insertion of alkyne into the Ru−C bond. The substituent effect in the complex ($\rho = -1.6$) suggests that, as in the palladium case,[7] the nucleophilic attack of the phenyl orthoruthenated carbon at a triple bond α-carbon plays a significant role in the transition state. Lower

Scheme 5

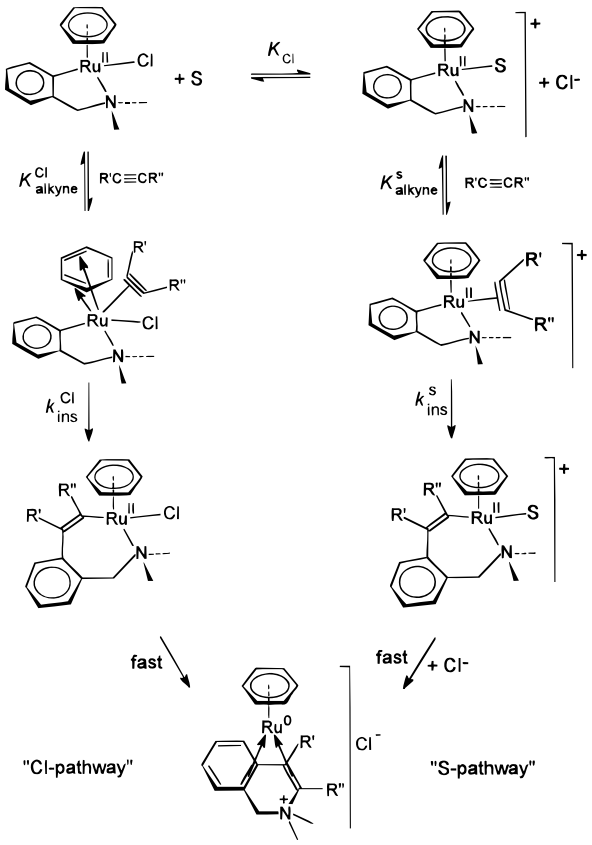

reactivity of the electron-poor alkynes (Table 4), whereas the electron-rich complexes **1** react faster than the electron-poor ones, indicates that the insertion may be considered as a concerted process; i.e., the Ru^{II} attack at the β-carbon occurs also in the transition state. This aspect of alkene and alkyne insertion reactions into the M−C bonds has been discussed in detail in our previous publications.[7,9] Thus, there is a hope that the alkyne insertion may occur with retention of the configuration of the Ru-bound chiral carbon, as observed on interaction of the enantiomeric cyclopalladated 8-ethylquinoline complex with alkynes.[20]

The fact that the bond making constitutes the transition state is supported by the values of enthalpies of activation $\Delta H^{\ddagger}$ which are not large and fall in the range 63−73 kJ mol^{-1}. These are only slightly higher than those observed for palladium complexes **5** (Table 3). At the same time the entropies of activation $\Delta S^{\ddagger}$ are less negative for complexes **1** indicative of a looser transition state in the ruthenium case. A plausible reason for that is the six-coordinated environment around Ru^{II} in contrast to the four-coordinated one in the case of the square-planar Pd^{II} complexes. Thus, there seems to be more freedom for alkynes in the coordination sphere of d^6 Ru complexes compared to d^8 Pd complexes. Curiously, the same idea has recently been put forward intuitively,[4b] without conclusive physicochemical evidence.

The insertion of alkyne is followed by the reductive elimination step to afford the final products **4**. Its rate is probably much faster than the rate-limiting insertion. We observed the monoexponential kinetics in all cases but for the reaction of DMAD with **1a**. In the latter

(18) Ryabov, A. D.; Kuz'mina, L. G.; Polyakov, V. A.; Kazankov, G. M.; Ryabova, E. S.; Pfeffer, M.; van Eldik R. *J. Chem. Soc., Dalton Trans.* **1995**, 999.

(19) Koelle, U.; Rietman, C.; Tjoe, J.; Wagner, T.; Englert, U. *Organometallics* **1995**, *14*, 703. See also refs 12.

(20) Spencer, J.; Pfeffer, M. *Tetrahedron*: *Asym.* **1995**, *6*, 419.

case, two steps were detected, the spectral changes for the second one being less pronounced. At present, it is difficult to conclude whether we observed the second reductive elimination step or routine decomposition of the final isoquinolinium complex **4**. This question is currently under investigation.

"Cl-Pathway". The only straightforward information concerning the "Cl-pathway" is that it is by 2 orders of magnitude slower than the solvolytic one for complex **1a**. Additional information is kinetically unattainable, since precision in evaluation of the rate constant k_{Cl} by fitting the experimental data to eq 2 is low. However, this pathway is encouraging from the mechanistic standpoint because it involves a rearrangement at a coordinatively saturated metal center with η^6-bound benzene. The "Cl-pathway" depicted in Scheme 5 is one of the possibilities. Its key feature is the precedented[21] reversible $\eta^6 \rightarrow \eta^4$ isomerization of the coordinated benzene which opens a room for either simultaneous or subsequent alkyne coordination. The following steps may match those in the dominant solvolytic pathway. Involvement of the $\eta^6 \rightarrow \eta^4$ isomerization allows one to avoid the mechanistic pattern suggested recently for reactions of alkynes with nickelacycles[8] according to which the preequilibrium coordination occurs without generation of the vacant site, with an increase in the coordination number of the nickel(II) complex by one unit. In fact, the seven-coordinated Ru(II) intermediate does not seem convincing.

The other mechanistic possibility of the "Cl-pathway" principally involves dechelation of the amine ligand. This route is also possible for complexes **5**, and such a possibility was in fact analyzed in much detail previously.[7,9] It was, however, rejected for the lack of conclusive evidence. We believe that in the case of d^6 Ru(II) complexes the pathway involving the Ru−N bond cleavage is even less probable than in the case of the d^8 Pd(II) species.

In conclusion, this study revealed that organometallic complexes of different metal nature containing the σ-M−C bond may follow synthetically relevant reactions with alkynes via a similar mechanism. The only principal difference observed in the case of d^6 Ru^{II} and d^8 Pd^{II} complexes concerns the mode of creation of an easy access of alkyne into a coordinative sphere of the two metals which is dictated by the chemical structure of the corresponding, respectively, monomeric and dimeric starting compounds.

Acknowledgment. We are grateful to Dr. A. V. Larin for writing the computer program and to the Alexander von Humboldt Foundation for donation of a Shimadzu UV-160A spectrophotometer.

Appendix

Equation 5 was derived taking into account the following equations: (i) the dissociation of LiCl driven by K_{LiCl}, (ii) the dissociation of complex **1** driven by K_{Cl} (Scheme 4), (iii) the mass balance equations for both LiCl and **1**, and (iv) the charge balance equation A1, which indicates that the total amount of cations and anions formed should be equal.

$$[Li^+] + [Ru_s] = [Cl^-] \tag{A1}$$

A combination of the corresponding expressions for the dissociation constants and the mass balance equations gives eqs A2 and A3.

$$[Li^+] = \frac{K_{LiCl}[LiCl]_t}{K_{LiCl} + [Cl^-]} \tag{A2}$$

$$[Ru_s] = \frac{K_{Cl}[\mathbf{1}]_t}{K_{Cl} + [Cl^-]} \tag{A3}$$

Substitution of eqs A2 and A3 into eq A1 and final rearrangement of the resulting equation leads directly to eq 5.

Supporting Information Available: Complete tables of bond distances and bond angles, positional parameters and their standard deviations, and general (U) and refined (β) displacement parameters (6 pages). Ordering information is given on any current masthead page.

OM960674B

(21) Davis, R.; Kane-Maguire, L. A. P. In *Comprehensive Organometallic Chemistry*, Wilkinson, G., Stone, F. G. A., Abel, E. W., Eds., Pergamon Press: Oxford, New York, 1982; Vol. 3, pp 953−1077.